Appendix

Table of Contents

List of Supplementary Files

Appendix – Supplemental Text, Figures and Tables

Supplementary Data 1 – A Microsoft Excel file containing Growth Rate, Flask, Generations, CCD of each experiment.

Supplementary Data 2 – A Microsoft Excel file containing mutations detected for each of the isolated clones across the different experiments.

Supplementary Data 3 – Transcriptomic analysis – expression level and differentially-expressed genes for each strain and across the set >6. Also, the genes in each modeling and COG category are included in this file.

Text

Characterization of the Evolution Process and the Endpoint Strains

It is assumed that the initial jumps in growth rate (from the first to second flask) observed in the ALE experiments are from the physiological adaptation to continual exponential phase growth. No increase in growth rate is expected due to a potential beneficial mutation until approximately 8-10 days into any experiment given the initial growth rate of the wild-type, the growth rates observed over the first half of the experiment, and assuming one cell was present with the higher growth rate at the start of the experiment.

To identify points in time where mutations benefitting growth rate (i.e., causal mutations) might have occurred and fixed in the individual populations, an analysis was performed to find regions where the fitness increased significantly over a short period of time for each population (i.e., "jumps" in the fitness). Briefly, a so-called 'jump finding algorithm' was developed and used to perform a monotonically increasing piecewise-cubic fit of the data. Regions with slopes larger than a threshold were considered 'jumps' (see Methods). The jumps found in each of the evolved populations are given in Supplementary Table 1. Every independent population had an initial growth rate jump of 1.11-1.16 fold. Following this initial jump, the growth rates of each population diverged (Figure 1). All experiments had at least two jumps identified, with two experiments having three. The initial jump region for experiment 4 differed from the other experiments as it apparently had a longer region of growth at the initial rate than the others, thus the start of the jump region was later in the evolution and subsequently it had the smallest increase in fitness. A sensitivity analysis was performed on the key parameters used to find jumps and it was found that the width of each jump region is sensitive to the slope threshold and increasing the number of spline segments will find more jumps. However, the increase in fitness of the first jumps identified using the developed jump finding algorithm was relatively

insensitive to these parameters. Changes to the minimum derivative needed to call a jump were as follows: A 50% decrease in derivative led to 1 additional jump found at the end of ALEs 5, 6, and 7. These jumps, from visual inspection, are not actual changes in growth rates but rather artifacts of the noise in measurement. A 50% increase in derivative led to the loss of 2 jumps, the second jump in ALE 9 and the last jump in ALE 10. Similarly, increases in the number of knots used led to identification of fluctuations within the noise range as jumps. This algorithm conservatively calls jumps such that the number of fitness jumps found should always be less than the number of actual jumps in fitness.

Analysis of Mutations Identified in the Evolved Strains

The genes that were found to be mutated most frequently were *pyrE/rph*, *rpoB*, *hns/tdk*, *corA*, *iap*, *ygaZ*, and *metL* and were found in 8, 8, 7, 3, 2, 2, and 1 of the experiments, respectively. Each of the genes and mutations were analyzed in more detail:

- The *pyrE/rph* ∆82bp deletion was observed in every sequenced clone. This exact mutation has been previously observed and it has been hypothesized to affect expression of orotate phosphribosyltransferase (i.e., the *pyrE* gene product) under minimal media conditions, counteracting a pyrimidine deficiency inherent to K-12 (1, 2). It is thought that the expression change occurs as a result of moving the stop codon of *pyrE* closer to an attenuating loop. This was the only recurring identical mutation found in every clone sequenced, including those sequenced before an observable jump in fitness was seen. Given the hypothesized mechanism for the mutation's occurrence, the length (82bp) of the deletion is highly conserved. This mechanism involves DNA polymerase slippage during replication, attributable to two flanking identical 10 bp repeat regions (2). This provides an explanation for the frequency at which this mutation

was observed and its early onset (likely before it fixed in the entire population, see further analysis below).

- The *rpoB* gene codes for a subunit of RNA polymerase and plays an integral role in binding to sigma factors via a highly conserved hydrophobic flap (3). Transcription initiation is highly dependent on *rpoB* activity and thus alterations to its function could be far reaching. *rpoB* mutations were observed in every ALE experiment after the first identified jump in fitness. A mutation in *rpoB* persisted until the end of each evolution, except in one strain that was identified as a hypermutator (experiment 7), and which possessed a mutation in a different RNA polymerase subunit, *rpoC*. Of the *rpoB* mutations, six unique SNPs were identified (Table 2). *rpoB* and the *pyrE/rph* mutations were the most dominant mutated genetic regions observed, and occurred following the first jump. The *rpoB* mutations E672K (GAA→AAA) and P1100Q (CCG→CAG) were found in multiple experiments, three and two, respectively, and persisted in all subsequent clones analyzed. The co-occurrence of *rpoB* E672K and *ygeW* S200R in experiments 5 and 9 suggest a potential cross contamination during experimentation. However, the same *rpoB* E672K mutation was found in experiment 3, but was not accompanied by the *ygeW* S200R SNP. As previously described, experiment 9 was started 14 days before experiments 3 and 5, thus a cross-over from experiment 9 growing at a significantly faster rate than experiment 5 likely explains this co-occurence. No clone from experiment 9 was found to have the *rpoB* E672K mutation without the *ygeW* S200R SNP, thus this does not definitively point to cross-over into experiment 3, but the possibility cannot be discounted.
- The intergenic region between *hns/tdk* was found mutated in all of the experiments except for the experiment where a hypermutating strain was dominant. Insertion sequences (IS) are regions of DNA that have a propensity to replicate and insert

themselves into new sites along the genome based on sequence homology (4). IS elements have been shown to have multiple potential effects from enhancement of transcription, activation of cryptic genes, and instigation of large scale re-arrangements of the genome (5-7). The *hns* gene was found to be significantly up-regulated in the strains that harbored the IS elements (all except the hypermutator clones, see transcriptomic analysis below). As the first jump in fitness was dominated by *rpoB* and *pyrE/rph* mutations, the second was dominated primarily by IS element insertion into the intergenic region of *hns/tdk* (except experiment 9, where the mutation was detected after a later jump). Of all of the *hns/tdk* mutations, only one was identical in strains isolated from experiments 5 and 10.

- The *corA* gene is responsible for a nickel, cobalt, and magnesium ion transporter along the inner membrane (8). Five unique mutations in *corA* were observed over the course of three independent ALE experiments. Of the five mutations, there were 3 deletions (2 in-frame), one 21 bp duplication, and one SNP. In experiments 4 and 5, mutations detected in *corA* were later replaced by different mutations in *corA* in subsequent clones. In experiment 10, a 21 bp duplication was detected, but was not found in later clones, likely due to clonal interference.
- The *iap* gene codes for an aminopeptidase alkaline phosphatase isozyme conversion protein that is thought to be membrane associated and act in the periplasm (9). It is worth noting that an identical mutation, an IS5 element insertion, was observed in *iap* in the final clone sequenced from both experiments 6 and 9. Since these clones did not share any addition mutations except the 82bp deletion in pyrE/rph, it is very likely that this identical mutation arose independently. Furthermore, a missense SNP in *iap* was also observed in the hypermutator lineage

- The *ygaZ* gene encodes for a subunit of an inner membrane L-valine efflux transporter (4, 8). Four unique mutations, all in coding regions and all likely to cause gene inactivation via frameshifts or premature protein truncation, were observed across three ALE experiments. In experiment 3, an IS element insertion was detected in *ygaZ* and subsequently replaced by an out of frame deletion of 10bp when clones from later in the experiment were analyzed. Experiment 10 had a 19bp duplication. None of these mutations were found immediately after the first fitness jump.
- The *metL* gene encodes the subunit of the homodimer aspartate kinase / homoserine dehydrogenase. It is involved in the pathways used to produce lysine, homolysine, methionine, and threonine (8). Two mutations in *metL* were observed in one experiment (experiment 10); a 1 bp frameshift deletion near the middle of the gene (i.e., at bp 1338 out of 2433 nucleotides) and a SNP 12 amino acids from the C-terminus. The latter replaced the former in the final clone sequenced.

The co-occurrence of jumps and mutations identified in each of the experiments was analyzed in more detail. The first jump in fitness was dominated by SNPs in *rpoB* and the 82bp deletion in the intergenic region of *pyrE/rph*. Both genetic regions were found to be mutated in every experiment. Additionally, clones were isolated from four experiments that appeared to have a region of stable observed growth rate at the beginning of the initial jump region (Figure 3). Each one of these four contained the 82bp deletion and only one of the clones had any additional genetic changes (from experiment 6). Furthermore, the frequent occurrence of mutations in the intergenic region of *hns/tdk,* only ever detected after a second jump, also points to mutational consistency across the evolution experiments. Therefore, the dominance of these two mutations prompted further examination of their impact on fitness (see below). More variation was seen when analyzing newly observed mutations after the second and third jump in fitness (Table 2).

Analysis of Reproducibility for Key Mutations Which Enable Increased Fitness Phenotypes

The three reconstructed strains were grown and evolved again on a shorter time scale to show that the key mutations tested were causal. The initial growth rates of the three reconstructed strains were found to be 0.82±0.02 hr^{-1}, 0.85±0.06 hr^{-1}, and 0.85±0.04 hr^{-1} for the *rpoB* E546V, *rpoB* E672K, and *pyrE/rph* Δ82 strains, respectively. Mimicking what was seen in the initial ALE experiment, the growth rate of all of the strains increased significantly after the first flask. This physiological adaptation increased the growth rates to 0.890±0.022 hr^{-1}, 0.915±0.023 hr^{-1}, and 0.936±0.032 hr^{-1}, respectively, a change of 0.07 hr^{-1}, 0.07 hr^{-1}, and 0.09 hr^{-1} as compared to a 0.15hr^{-1} increase for the wild-type strain in the initial ALE.

The fitness trajectories of the validation ALE experiment were analyzed, as before, with the jump finding algorithm and used to identify points in the experiments from which to isolate clones for whole-genome resequencing. The average fitness increase for the validation ALE was 1.14-1.19 fold for all of the nine experiments, and each of the experiments underwent one primary jump in fitness according to the parameters of the developed algorithm (see Methods). Supplementary Table 2 provides the fitness increases for each of the jumps. Clones were isolated from each experiment pre- and post- jump region as well as a few additional locations (Supplementary Figure 4).

The appearance of a mutation in the intergenic region of *pyrE/rph* was highly reproducible. Of the six experiments started with one of two *rpoB* mutant strains, the characteristic Δ82bp deletion in the intergenic region of *pyrE/rph* was observed in four of the six (in one strain, a SNP in *rffD* was also detected with the *pyrE/rph* mutation). Interestingly, a different mutation, a

Δ1bp deletion in the intergenic region of *pyrE/rph,* was detected in one of the six experiments. This suggests that this mutation may have a similar effect given that it was also isolated after the initial jump. Based on the DNA sequence in the region, a deletion of 82bps is the most likely length (1). The endpoint populations of the validation ALE were also probed for the Δ82bp deletion using PCR (Supplementary Figure 5). Of the six experiments that originated from reconstructed *rpoB* strains, all showed evidence of obtaining the Δ82bp deletion. None of the endpoints showed complete penetration of the mutation when compared to the PCR results of the experiments originating with the Δ82bp deletion. No reversion of the Δ82bp deletion was expected nor was any evidence thereof observed. Thus, the Δ82bp deletion was highly reproducible, was detected in most strains using resequencing, and in all populations using PCR. In the one experiment where a *pyrE/rph* mutation was not detected through whole-genome resequencing, a mutation was found in *metL* and in the intergenic region between *xdhD/xanQ*. A stop codon was introduced about halfway through the coding region of *metL* in the validation ALE experiment. The primary ALE experiment showed a Δ1bp deletion in roughly the same location (residue location 424 versus 446 out of 810). Both mutations would presumably result in a loss of function of the *metL* gene.

The appearance of a mutation in *rpoB* was highly reproducible in the evolved strains starting from a Δ82bp *pyrE/rph* mutant. Whole-genome resequencing of clones isolated after a jump in fitness revealed that mutations in *rpoB* occurred in two out of three experiments. Both mutations were distinct from those found in the primary ALE experiment (Table 4). In one evolution, no mutations were found in a clone isolated after the initial jump in population growth rate. Furthermore, a single mutation was seen in an interim clone in experiment #9 of the validation ALE in the intergenic region between *hns/tdk*, consistent with the type observed in the primary ALE (i.e., an IS element insertion). It did not persist in the final clone isolate and

the validation ALE was terminated after one fitness jump. As the *hns/tdk* mutation was only observed during jump 2 and 3 in the primary ALE experiment, it is not unexpected that it could be outcompeted by an *rpoB* mutant that was shown to dominate the initial jump in fitness in the primary ALE.

Integrated Genome-scale Modeling

Each of the gene sets in the pared gene group analysis formed by the combined COGs annotations and modeling predictions were analyzed in detail. The findings for each are described in the following paragraphs.

Most of the genes in the Utilized ME and Amino acid metabolism (E) COG categories are involved with the biosynthesis of a number of amino acids including threonine (*thrBC*), methionine (*metE*), selenocysteine (*selA*), asparagine (*asnA*), arginine (*argBCEGHI*), histidine (*hisCDG*), lysine (*dapBD*, *lysC*), glutamate (*gdhA*), cysteine (*cysKM*), and tryptophan (*trpAB*), with two additional genes in the glycine cleavage system (*gcvHT*) present. In the Utilized ME and Transcription (K) COG categories, all subunits of the RNA polymerase sigma 70 holoenzyme are present (*rpoA*BCD), which targets promoters related to exponential growth. *rpoZ* and the elongation factor *greA* and termination factors *nusG* and *nusA* are also present. The Utilized ME and Translation (J) COG categories contain many ribosomal genes (20 from the 50S subunit and 13 from the 30S subunit), 6 tRNA synthases, 6 stable RNA modification and processing enzymes, several translation initiation and elongation factors, and *map* for N-terminal methionine cleavage. All but two Utilized ME genes in the Protein maturation (O) COG category are in the DnaK-DnaJ-GrpE, GroEL-GroES, and Trigger Factor chaperone systems, which aid in folding newly synthesized cytosolic proteins. Synthesis of the functional proteome is the clear trend in all of these genes.

Though not shown in Figure 7B, one COG category, Carbohydrate metabolism, was enriched among the Non-utilized ME genes. Many of these genes are involved with the uptake and utilization of alternative carbon sources not present in the media, including ribose (*rbsBDK*), fructose (*fruK*), galactitol (*gatY*), and hexuronates (*kdgK*, *uxaAC*, *uxuAB*). While these carbon sources are not present in the media, their up-regulation may be a side-effect of the general up-regulation of carbon catabolism. Interestingly, glucokinase (*glk*) is up-regulated as well, though *E. coli* (and the ME-Model) typically uses the PTS system for glucose import, indicating that the evolved strains to some extent may import glucose by proton symport. Additionally, *eda* from the Entner-Doudoroff pathway is up-regulated, indicating the evolved strains may be using this alternative glycolytic pathway. Recent work has suggested that while the canonical EMP pathway has higher ATP yield, the ED pathway is more thermodynamically favorable, and has a lower protein cost, which could support a higher flux (10). Oddly, methylglyoxal synthase (*mgsA*), which catalyzes the formation of the highly toxic methylglyoxal, is up-regulated. The enzyme is lowly abundant, however, and can help to regulate the abundance of sugar phosphates (11). The remaining genes in this category catalyze reactions in central carbon metabolism that are predicted to be active in the ME-Model, but which utilize alternative isozymes (*tktA*, *glpX*, *gmpA*, *talB*), highlighting the need to better understand isozyme usage *in vivo* and preferences in the model.

Several sets of genes were indicated in the Outside scope ME genes and COGs annotation intersection. COG categories with increased expression include Replication and repair (L), Intracellular trafficking and secretion (U), and protein maturation (O). Those with decreased expression include Cell wall/membrane biogenesis (M), Signal transduction (T), and Function unknown (S).

Many of the genes essential for DNA replication have increased expression, including a subunit of DNA polymerase (*dnaZ*), topoisomerase (*parC*), and both subunits of DNA gyrase (*gyrAB*). Up-regulation of these genes could be due to the multiple replication forks required for replication at higher growth rates (12). In addition to genes clearly important for cellular growth, many DNA repair genes are up-regulated, including *mutS*, *mutM*, *recA*, *ssb*, and *uvrD*. These will presumably alter the mutation rate, affecting the dynamics and stability of the evolution.

The up-regulated Outside scope ME genes involved with protein maturation are largely protein folding chaperones or involved in resolubilizing or degrading aggregated or mis-folded proteins. Unlike the three canonical protein folding chaperones that are represented in the ME-Model and up-regulated, the chaperones not represented in the model are co-chaperones or aid in folding, but are not essential for the process (e.g., *htpG*, *djlA*, and *ibpA*). As proteins spontaneously aggregate and mis-fold, it is conceivable that increased enzyme synthesis would require proteins to assist in their degradation or re-folding; up-regulated genes with these functions include *lon*, *hslVU*, *clpB*, *htpX*, and *ybbN*.

The down-regulated Outside scope ME genes involved with Cell wall/membrane biogenesis (M) include a number of genes with repair and degradation functions, including membrane repair (*blc*), murein/peptidoglycan degradation (*nlpD*, *mepEHS*), and a protease (*ompT*). Genes related to various stress responses, including biofilm formation (*csgG*), acid stress (*slp*), hyposmotic stress (*ynaI*), and a few genes with unknown function (*yfiB*, *yfdH*, *yegX*), are also present. The down-regulated Outside scope ME genes involved in Signal transduction (T) include a number of stress sensors and regulators, including those governing Mg+ levels (*phoQ*), motility and quorum sensing (*ydiV*), phosphate starvation (*phoH*), oxidative stress

(*msrC*), and a few genes with unknown regulatory functions (*ylaB, yedV, yjcC*). Additionally, *aceK* is present, which controls the activity of isocitrate dehydrogenase and the split between the TCA and glyoxylate cycles, which is potentially related to some of the TCA expression shifts observed. The Outside scope ME genes in the Function unknown (S) COG still have ill-defined functions. Generally, many of the down-regulated Outside scope ME expression changes support down-regulation of non-growth functions.

Table S1 – Regions for each of the populations where fitness increased significantly

	1st Jump			2nd Jump			3rd Jump		
Experiment Number	Start (CCD)	Length (CCD)	Growth Increase	Start (CCD)	Length (CCD)	Growth Increase	Start (CCD)	Length (CCD)	Growth Increase
3	8.70E+10	3.16E+12	0.16	4.28E+12	2.57E+12	0.04			
4	8.34E+11	1.78E+12	0.11	3.11E+12	1.65E+12	0.04			
5	4.67E+11	2.95E+12	0.14	4.71E+12	4.29E+12	0.06			
6	0	2.92E+12	0.15	3.54E+12	1.56E+12	0.04			
7	6.18E+10	2.73E+12	0.16	3.62E+12	2.40E+12	0.11	6.85E+12	1.66E+12	0.03
8	0	2.76E+12	0.13	3.36E+12	2.48E+12	0.06			
9	7.70E+10	3.20E+12	0.16	5.90E+12	1.83E+12	0.02	9.24E+12	2.28E+12	0.03
10	9.29E+10	2.91E+12	0.12	5.39E+12	3.80E+12	0.06			
Average	1.98E+11	2.87E+12	0.14±0.02	4.28E+12	2.93E+12	0.06±0.03	8.05E+12	1.97E+12	0.03

Table S2 – Regions for each of the populations where fitness increased significantly for the validation ALE

	1st Jump		
Experiment Number	Start (CCD)	Length (CCD)	Growth Increase
1	7.07E+11	1.05E+12	0.06
2	7.17E+11	9.80E+11	0.07
3	5.24E+11	1.62E+12	0.09
4	8.03E+11	1.37E+12	0.07
5	1.14E+12	9.76E+11	0.08
6	7.84E+11	1.36E+12	0.07
7	7.18E+11	1.13E+12	0.05
8	1.10E+12	9.94E+11	0.06
9	8.38E+11	1.37E+12	0.06
Average	8.15E+11	1.21E+12	0.07

Figures

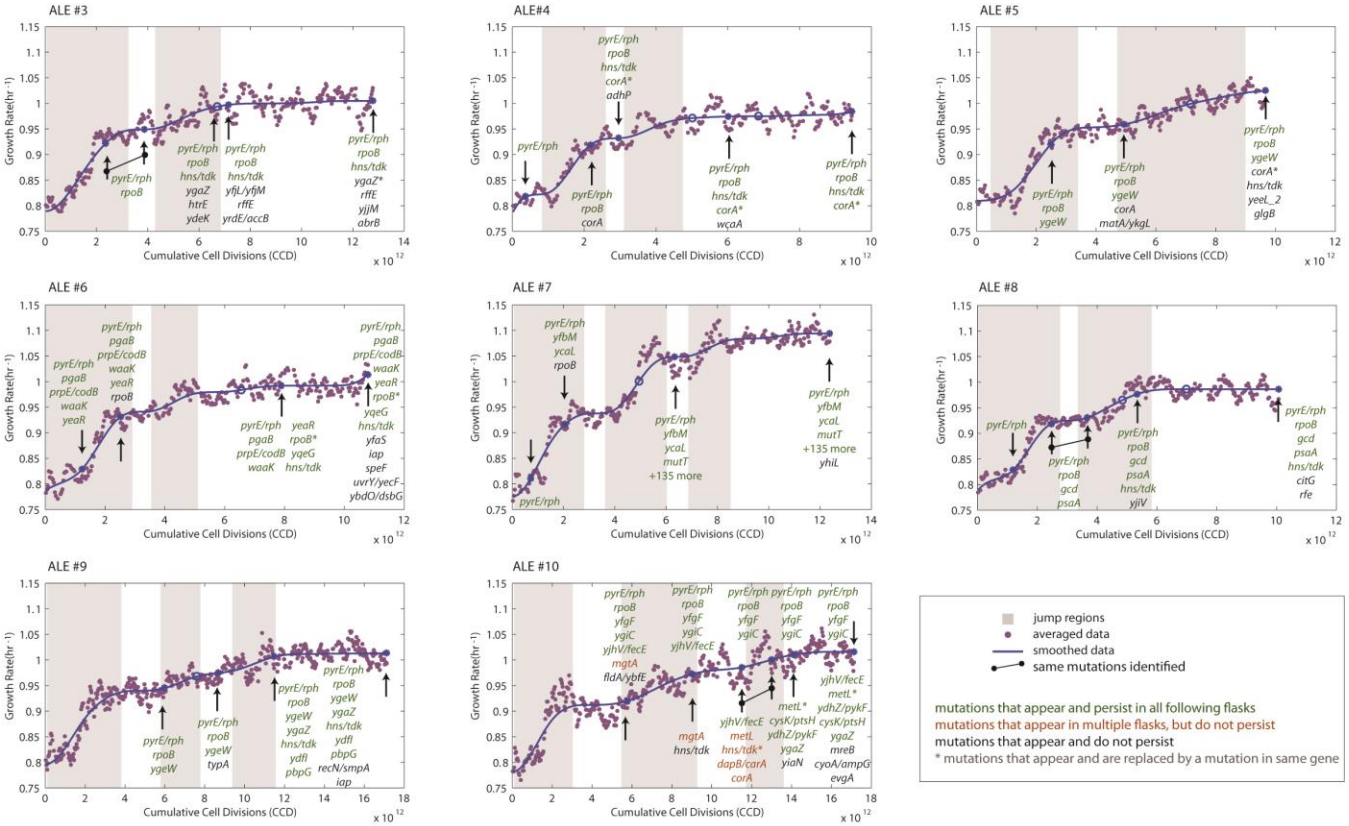

Figure S1: Plots of the identified jump regions and mutations found in clones isolated at various points along the ALE experiments. Jump regions were identified by first smoothing the data using a cubic spline interpolation then finding regions where the derivative was above a certain threshold. Jumps identified that were not longer than 4 days were not accepted. Jumps were ranked according to their increase in growth rate and the length of jump, favoring short jumps with large increases. The green dots indicated locally averaged data before smoothing was applied.

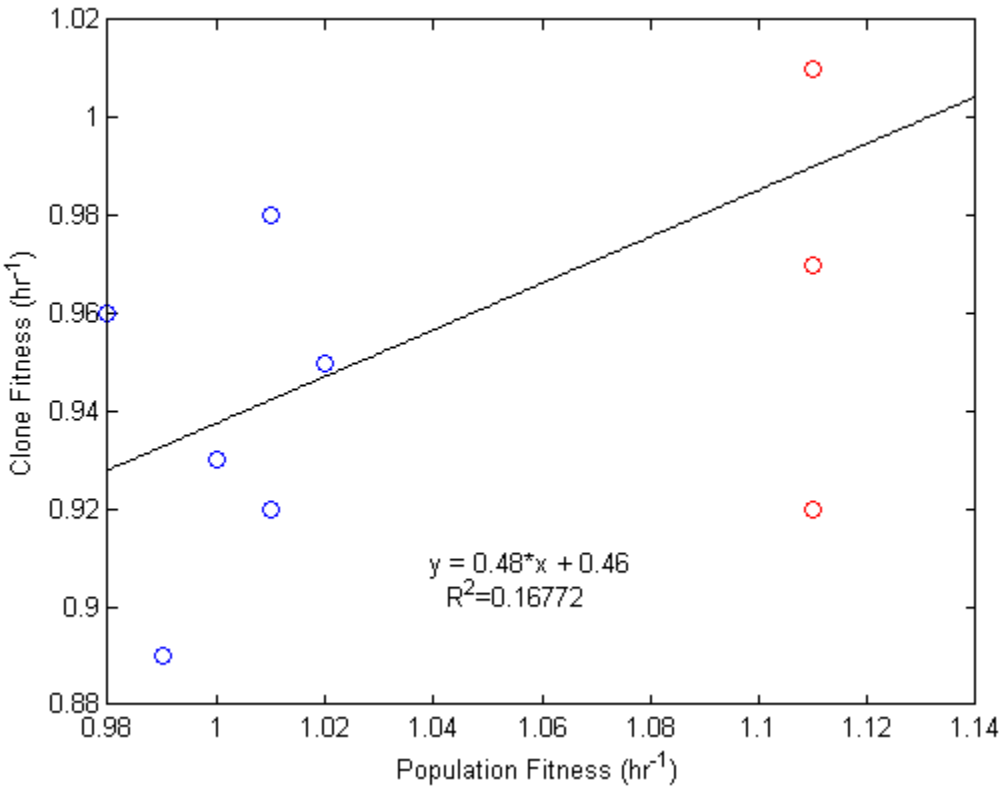

Figure S2: The relationship between the populations and the clones isolated from the populations are weakly correlated. Red circles correspond to hypermuator clones and blue to non-hypermutator clones. It is plausible that isolating a less-than-optimal clone from a hypermutator population could lead to the weak correlation.

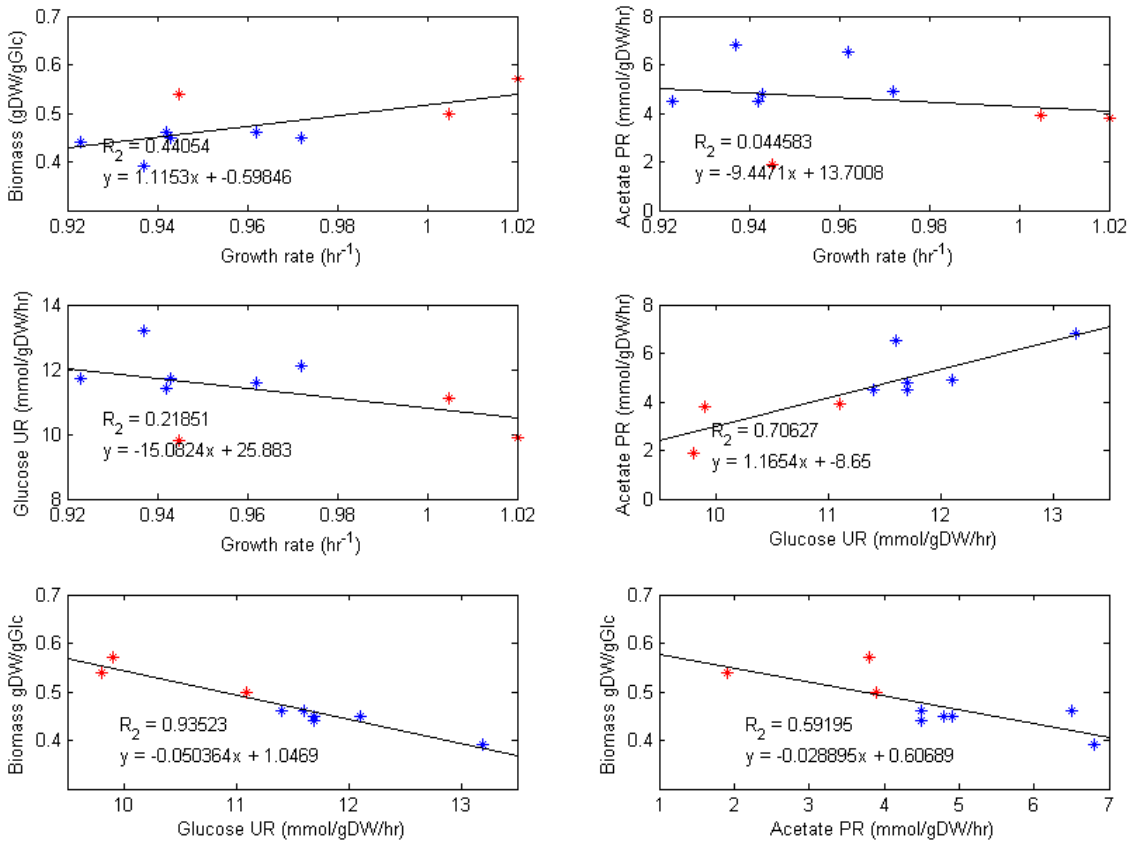

Figure S3: Pairwise comparisons of all phenotypic data were made for each endpoint isolate. Biomass Yield vs Glucose uptake rate (GUR) and GUR vs Acetate production rate were the most highly correlated.

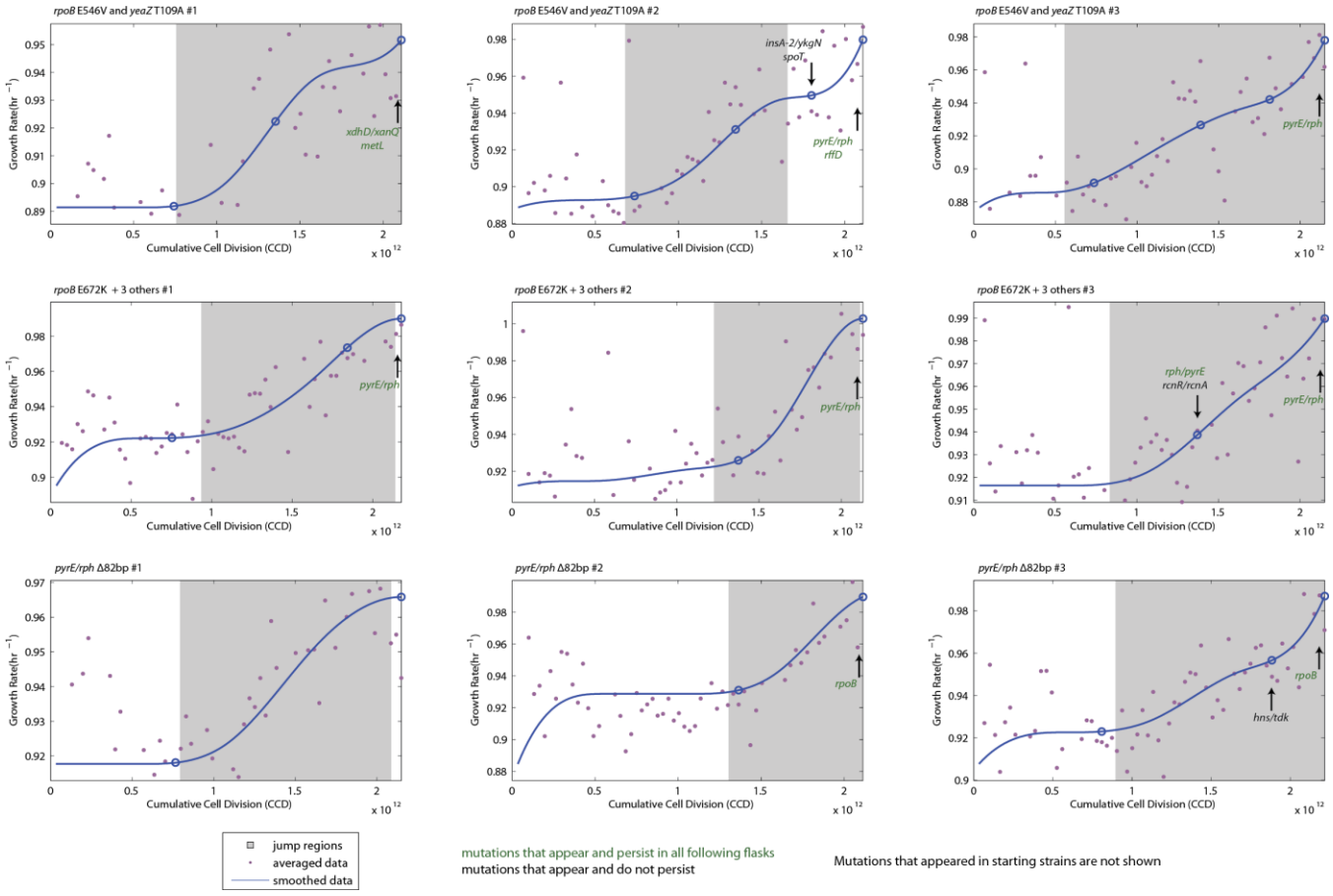

Figure S4: Validation ALE Jumps and Sequences - Prepared in the same fashion as Supp Fig 1 but with the dataset from the validation ALE.

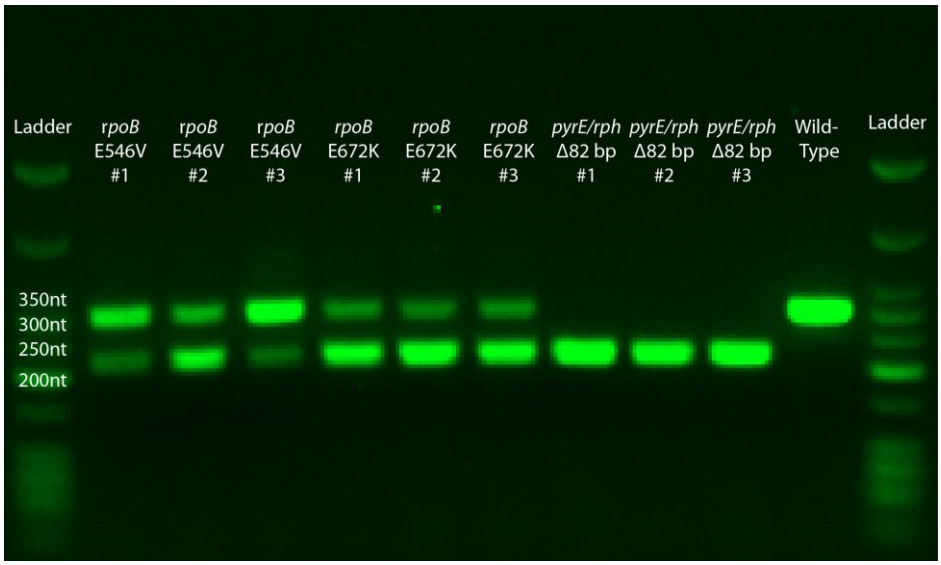

Figure S5: Δ82bp deletion in pyrE/rph penetration by PCR - Populations from the final flask of the validation ALE were probed for the presence of the Δ82bp deletion in pyrE/rph. The upper band shows wild-type genotype and the lower band shows a deletion in pyrE/rph. Low molecular weight ladders were run on the outermost lanes (N0474S from Bio Labs). When clones were sequenced from these populations, rpoB E546V #1 showed no mutations in pyrE/rph and rpoB E546V #3 showed only a Δ1bp deletion in pyrE/rph which would not be resolved from the wild-type band in the gel. Though not observed in all the clones, the PCR results clearly show that a ~Δ82bp deletion in pyrE/rph exists in all the final populations. Based on the relative intensities of the bands, the degree to which the 82bp deletion has penetrated the culture varies. Specifically, in the populations where the clones did not show the Δ82bp deletion, the wild-type band shows greater intensity than the mutant band, thus corroborating why we did not see the Δ82bp deletion in the clone sequences.

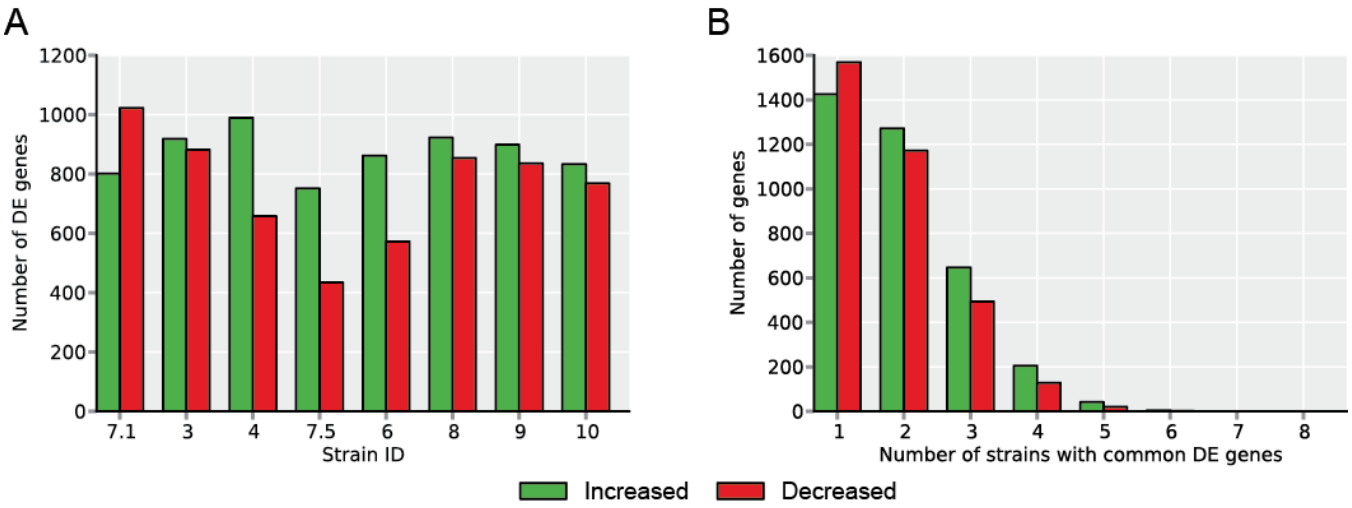

Figure S6: Transcriptomic Data: Enriched Differentially Expressed Protein coding Genes from Evolved Strains. (A) The Differentially expressed genes from each strain. (B) Distribution of differentially expressed genes if expression was randomized.

References

1. **Conrad TM, Joyce AR, Applebee MK, Barrett CL, Xie B, Gao Y, Palsson BO.** 2009. Whole-genome resequencing of Escherichia coli K-12 MG1655 undergoing short-term laboratory evolution in lactate minimal media reveals flexible selection of adaptive mutations. Genome Biol **10:**R118.

2. **Jensen KF.** 1993. The Escherichia coli K-12 "wild types" W3110 and MG1655 have an rph frameshift mutation that leads to pyrimidine starvation due to low pyrE expression levels. J Bacteriol **175:**3401-3407.

3. **Kuznedelov K, Minakhin L, Niedziela-Majka A, Dove SL, Rogulja D, Nickels BE, Hochschild A, Heyduk T, Severinov K.** 2002. A role for interaction of the RNA polymerase flap domain with the sigma subunit in promoter recognition. Science **295:**855-857.

4. **Bukhari AI, Shapiro JA, Adhya SL, Cold Spring Harbor Laboratory.** 1977. DNA insertion elements, plasmids, and episomes. Cold Spring Harbor Laboratory, Cold Spring Harbor, N.Y.

5. **Barker CS, Pruss BM, Matsumura P.** 2004. Increased motility of Escherichia coli by insertion sequence element integration into the regulatory region of the flhD operon. J Bacteriol **186:**7529-7537.

6. **Hall BG.** 1999. Transposable elements as activators of cryptic genes in E. coli. Genetica **107:**181-187.

7. **Umeda M, Ohtsubo E.** 1989. Mapping of insertion elements IS1, IS2 and IS3 on the Escherichia coli K-12 chromosome. Role of the insertion elements in formation of Hfrs and F' factors and in rearrangement of bacterial chromosomes. J Mol Biol **208:**601-614.

8. **Riley M, Abe T, Arnaud MB, Berlyn MK, Blattner FR, Chaudhuri RR, Glasner JD, Horiuchi T, Keseler IM, Kosuge T, Mori H, Perna NT, Plunkett G, 3rd, Rudd KE, Serres MH, Thomas**

GH, Thomson NR, Wishart D, Wanner BL. 2006. Escherichia coli K-12: a cooperatively developed annotation snapshot--2005. Nucleic Acids Res **34:**1-9.

9. **Ishino Y, Shinagawa H, Makino K, Amemura M, Nakata A.** 1987. Nucleotide sequence of the iap gene, responsible for alkaline phosphatase isozyme conversion in Escherichia coli, and identification of the gene product. J Bacteriol **169:**5429-5433.

10. **Flamholz A, Noor E, Bar-Even A, Liebermeister W, Milo R.** 2013. Glycolytic strategy as a tradeoff between energy yield and protein cost. Proc Natl Acad Sci U S A **110:**10039-10044.

11. **Totemeyer S, Booth NA, Nichols WW, Dunbar B, Booth IR.** 1998. From famine to feast: the role of methylglyoxal production in Escherichia coli. Mol Microbiol **27:**553-562.

12. **Cooper S, Helmstetter CE.** 1968. Chromosome replication and the division cycle of Escherichia coli B/r. J Mol Biol **31:**519-540.